



UNIVERSITY OF LEEDS

This is a repository copy of *CEA-targeted nanoparticles allow specific in vivo fluorescent imaging of colorectal cancer models.*

White Rose Research Online URL for this paper:
<http://eprints.whiterose.ac.uk/84085/>

Version: Accepted Version

Article:

Tiernan, JP, Ingram, N, Marston, G et al. (6 more authors) (2015) CEA-targeted nanoparticles allow specific in vivo fluorescent imaging of colorectal cancer models. *Nanomedicine*. 1 - 9. ISSN 1743-5889

<https://doi.org/10.2217/NNM.14.202>

Reuse

Unless indicated otherwise, fulltext items are protected by copyright with all rights reserved. The copyright exception in section 29 of the Copyright, Designs and Patents Act 1988 allows the making of a single copy solely for the purpose of non-commercial research or private study within the limits of fair dealing. The publisher or other rights-holder may allow further reproduction and re-use of this version - refer to the White Rose Research Online record for this item. Where records identify the publisher as the copyright holder, users can verify any specific terms of use on the publisher's website.

Takedown

If you consider content in White Rose Research Online to be in breach of UK law, please notify us by emailing eprints@whiterose.ac.uk including the URL of the record and the reason for the withdrawal request.



eprints@whiterose.ac.uk
<https://eprints.whiterose.ac.uk/>

CEA-targeted nanoparticles allow specific *in vivo* fluorescent imaging of colorectal cancer models

James P Tiernan^{1,2}, Nicola Ingram¹, Gemma Marston¹, Sarah L Perry¹, Jo V Rushworth³, P Louise Coletta¹, Paul A Millner^{4*}, David G Jayne^{1,2*}, Thomas A Hughes^{1*±}

¹School of Medicine, University of Leeds, Leeds LS9 7TF, UK

²John Goligher Colorectal Unit, St James's University Hospital, Leeds, LS9 7TF, UK

³School of Allied Health Sciences, De Montfort University, Leicester LE1 9BH, UK

⁴School of Biomedical Sciences, University of Leeds, Leeds LS2 9JT, UK

*these authors have contributed equally

±corresponding author: Thomas A Hughes (Wellcome Trust Brenner Building, St James's University Hospital, University of Leeds, Leeds LS9 7TF, UK. tel +44 (0)113 3431984. email: t.hughes@leeds.ac.uk)

Running title: Tumour imaging *in vivo* using fluorescent CEA-targeted nanoparticles

Key words: dye-doped; silica nanoparticles; IVIS imaging; live tumour imaging; tumour markers; colorectal cancer

Abstract

Fluorescent imaging of colorectal tumour cells would improve tumour localisation and allow intra-operative staging, facilitating stratification of surgical resections thereby improving patient outcomes. We aimed to develop and test fluorescent nanoparticles capable of allowing this *in vivo*. Dye-doped silica nanoparticles were synthesised. Anti-CEA or control IgGs were conjugated to nanoparticles using various chemical strategies. Binding of CEA-targeted or control nanoparticles to colorectal cancer cells was quantified *in vitro*, and *in vivo* after systemic-delivery to murine xenografts. CEA-targeted, polyamidoamine dendrimer-conjugated, nanoparticles, but not control nanoparticles, allowed strong tumour-specific imaging. We are the first to demonstrate live, specific, *in vivo* imaging of colorectal cancer cells using antibody-targeted fluorescent nanoparticles. These nanoparticles have potential to allow intra-operative fluorescent visualisation of tumour cells.

Introduction

Colorectal cancer resections are based on operations that have been performed for over 100 years, involving a radical mesenteric basin resection encompassing primary tumour, vasculature and lymphatics [1]. However, this ‘one size fits all’ approach may be inappropriate in an increasing proportion of cases. Currently only ~35% of patients undergoing colorectal cancer resections have nodal metastases [2], yet all of them undergo this radical resection. National bowel cancer screening programmes have led to increases in diagnoses of small, early stage cancers, such as polyp and Dukes’ A cancers [3]. These are less likely to have nodal metastases therefore resection with radical lymphadenectomy could be regarded as over-treatment. On the other hand, some have suggested that patients with nodal metastases may benefit from even more radical resections [4]. Unfortunately, at present there is no accurate method for assessing nodal status pre- or intra-operatively. A further issue is that accurate localisation of small tumours during laparoscopic surgery, which is now in routine use in many centres [5], is especially problematic because of a lack of tactile feedback. These problems highlight the need for intra-operative tumour imaging that would aid tumour localisation, and could also allow intra-operative staging of nodal metastases and thereby allow surgeons to stratify resection radicality to each individual patient.

Laparoscopic surgery provides an ideal platform for intra-operative fluorescent imaging. Camera systems can be modified simply to provide excitatory light of various wavelengths and fluorescent signals and white-light images can be detected and overlaid on-screen for real-time surgical guidance [6]. While technologies required for physical imaging are relatively well developed, the biological and nanotechnological requirements have lagged behind. We have previously investigated which colorectal cancer biomarker is suitable in this context and have determined that the tumour marker CEA provides the best sensitivity and specificity for colorectal cancer detection and localisation [7]. We have now developed and validated a fluorescent nanoparticle that can target CEA to allow fluorescent tumour visualisation. The requirements for such a particle are challenging. The particle must be bright enough to allow detection through tissue, whilst remaining sufficiently small to pass

out of vasculature after intravenous delivery. Ideally, particles should have near-infrared emission wavelengths to increase tissue penetration and reduce auto-fluorescence [8]. Particles must also have acceptable biotoxicity profiles, and resist photobleaching. We have focused on dye-doped silica nanoparticles, which have potential to meet these criteria. For the dye, we used NIR-664, which is an iodoacetamide dye with suitable excitation and emission characteristics (672nm and 694nm respectively), as well as relatively good stability across different pH values and high quantum efficiency (23%) [9]. A number of studies have been published in which dye-doped silica particles have been investigated as agents to label cancer cells fluorescently [10-12]. However, a key concern is the non-specific binding potentially exhibited by particles when using some conjugations to antibodies, meaning that use of appropriate non-tumour targeted controls is critical. Here we show the first successful and robustly-controlled use of systemically-delivered, targeted fluorescent nanoparticles for live *in vivo* colorectal cancer imaging. This represents a key stage in development of clinically practical intra-operative fluorescent imaging for colorectal cancer.

Materials and methods

Nanoparticle manufacture

Protocols were carried out at room temperature using Sigma-Aldrich (USA) reagents unless otherwise stated. Protocols were modified from previous publications [10, 11, 13]. 'Wash' steps: nanoparticles were pelleted by centrifugation (11000g, 25min), resuspended in wash solution using ultrasound sonication, repelleted, and the supernatant discarded. 5mg NIR664 (Santa Cruz, USA) was dissolved in 6.25ml 1-hexanol, and 3.25µl (3-mercaptopropyl) triethoxysilane was added (stirred under nitrogen, 4h). 4.045ml Triton X-100 was added to 15ml cyclohexane, 1.6ml 1-hexanol, 2ml dye mixture and 960µl water (stirred, 5min). 200µl tetraethyl orthosilicate was added (stirred, 30min). 120µl 28% [w/w] ammonia hydroxide was added (stirred, 24h). 150µl tetraethyl orthosilicate was added (stirred, 30min). 20ml ethanol was added and mixture was divided into two equal volumes before centrifugation (11000g, 25min). Particles were washed in ethanol (x4). 4ml ethanol-suspended nanoparticles (2mg/ml) were stirred with 4% (3-aminopropyl)triethoxysilane (3h). Particles were washed in ethanol (x2), and once in 2-(N-morpholino)ethanesulfonic acid buffer (MES), pH 7, before resuspension in MES pH 7 at 2mg/ml.

Antibodies

Humanised anti-CEA monoclonal antibody A5B7 was supplied by the Cancer Research UK Biotherapeutics Development Unit (Clare Hall Laboratories, UK). This antibody was raised against purified human CEA from human metastatic colon tumour tissue [14], and has been used previously in human clinical trials of CEA-targeted therapies [15, 16] and in molecular pathology studies of human tissue [7]. Mouse monoclonal anti-digoxin IgG antibody (clone DI-22; Sigma-Aldrich, USA) was used as a negative, non-targeted, control.

Antibody conjugation

SMCC. 500µl 4.8mg/ml anti-CEA IgG antibody was added to 500µl 9.6mg/ml 2-mercaptoethylamine (2-MEA). The mixture was incubated at 37°C for 90min and then cooled rapidly on ice. 2-MEA was

then removed using a 100kDa spin centrifuge filter (Millipore, Billerica, USA); the mixture was centrifuged in 0.1M PBS (14000g for 2.5min) and the eluent discarded. This was repeated seven times. The concentrated antibody solution was then retrieved by gentle centrifugation with the tube inverted (1000g for 30s) and 0.1M PBS was added to make the total volume up to 500 μ l. The solution containing whole and reduced antibody fragments was reacted with nanoparticles immediately. 6mg of fresh sulfo-SMCC was added to 4ml 1mg/ml nanoparticles and stirred for 1h. The maleimide-activated particles were then washed twice in PBS (10000g for 15min) to remove unbound sulfo-SMCC, and were resuspended at 2mg/ml. The sample was split into two and 30 μ g of reduced anti-CEA or anti-digoxin was added to each tube. The reaction mixture was gently stirred for 2h and then washed twice with PBS (6000g for 15min). Finally, the particles were resuspended at 2mg/ml and 0.1% [w/v] BSA added. The finished nanoparticles were stored in the dark at 4°C.

PEG. A stock solution of 250mM NHS-PEG-maleimide (SM(PEG))₄ was made by dissolving 100mg in 680 μ l dimethyl sulfoxide (DMSO). 8 μ l of 250mM SM(PEG)₄ solution was added to 5ml of 2mg/ml nanoparticles and reacted for 30min with gentle mixing. Unreacted linker was removed by washing particles twice with PBS (pH 7.2, 10000g, 15min) and resuspending them in PBS at 2mg/ml. The sample was divided into two. 30 μ l of either anti-CEA or anti-digoxin IgG was added for each mg of nanoparticles. The reaction mixture was incubated for 2h with gentle mixing. The particles were then washed twice with PBS and resuspended at 2 mg/ml. 0.1% [w/v] BSA was added and they were stored in the dark at 4°C.

EDC. Nanoparticles were washed twice in DMF (10000g, 15min). They were then resuspended at 1mg/ml in 15ml 10% succinic anhydride dissolved in DMF. This was incubated under argon for 4h with gentle stirring. The carboxylated particles were then washed three times with distilled water. 10mg of carboxylated nanoparticles were suspended in 5ml 0.1M MES, 0.5M NaCl, pH 6.0, and 1.92mg EDC and 5.43mg sulfo-NHS were added. They were incubated for 15min with gentle mixing, after which the reaction was quenched by addition of 20mM 2-mercaptoethylamine (2-MEA). Excess reactants were removed by washing the particles twice with PBS (6000g for 10min) and resuspended

at 2mg/ml in 0.1M PBS. 10 μ g of either anti-CEA or anti-digoxin IgG was added for each mg of nanoparticles. The reaction mixture was incubated for 2h with gentle mixing. The particles were then washed twice with PBS and resuspended at 2mg/ml. 0.1% [w/v] BSA was added and particles were stored in the dark at 4°C.

PAMAM dendrimer. 41.7mg sulfo-NHS and 71.6mg N-(3-dimethylaminopropyl)-N'-ethylcarbodiimide were added to 1 μ mol polyamidoamine (PAMAM) dendrimer generation 4.5 (Dendritech, USA) dissolved in water, and the volume was made up to 1ml with MES pH 6 (stirred, 25min). 2mg nanoparticles in MES pH 7 were added (stirred, 25min). Particles were pelleted (16000g, 8min), and washed in MES pH 7 (x2). Samples were divided into two before addition of either 10 μ g of A5B7 anti-CEA antibody (CRUK, UK) or anti-digoxin IgG antibodies (Therapeutic Antibodies, UK). Particles and antibody were stirred (4h) before addition of 100 μ l 0.1M sodium hydroxide, pH 9.1. Particles were washed in 0.1M PBS pH 7.2 (x2) before resuspension in 0.1M PBS at 2mg/ml. 2% [w/v] BSA was added and particles were stored (4°C, dark).

Scanning electron microscopy (SEM)

Images were captured using LEO1530 (Zeiss, Germany) or FEI Quanta (FEI, USA) field emission SEMs.

Tissue culture, confocal microscopy and image analysis

Cell lines were obtained from ATCC (USA). LS174T, LoVo and HCT116 cells were cultured in Advanced MEM (ATCC), F12K Nutrimix and RPMI1640 (both Invitrogen, USA) respectively, supplemented with 10% FCS and 1% L-glutamine at 37°C in 5% CO₂. Cells were seeded onto glass coverslips (Cellpath, UK) for 24h. Cells were washed twice (PBS), fixed in 4% paraformaldehyde (30min), and washed in PBS (x3). Coverslips were incubated in 0.1% [w/v] BSA (30min) followed by PBS washes (x3). Coverslips were incubated with conjugated nanoparticles (1mg/ml in PBS) (1h, dark). Coverslips were washed in PBS (x3) and mounted using Depex (Waltham, USA). A Nikon A1R-A1 confocal microscope (Nikon, Japan) with NHS Elements software (v4.0) was used. For each

slide, cells were focussed in phase mode in the centre of one coverslip quadrant. Cy7 and phase filters were calibrated automatically for this first image only; settings (laser power and gain) were saved and used for all subsequent images. Phase/Cy7 z-stack images were captured for this first quadrant; distances between optical sections were chosen to allow similar numbers of sections for each line and the whole cellular depth to be included (0.5, 0.2 and 0.4 μm for LS174T, LoVo and HCT116 respectively). The microscope stage was then moved to another quadrant, focussed and examined under white light only (thereby minimising selection bias), and a further z-stack captured. This was repeated so five z-stacks were captured from each coverslip, from approximately each quadrant centre and one from the centre of the entire coverslip. Single optical sections to be analysed were taken from half way between base and top of the cells: at 5, 1.4 and 4.8 μm from the base for LS174T, LoVo and HCT116 respectively. Fluorescence was quantified using tiff images with ImageJ v1.42q (NIH Freeware, USA). Membrane fluorescence (per μm) was determined by measuring the cell circumference, masking the cytoplasm, and normalising to background. This procedure was followed for five z-slices per cell line/particle type. Maximum image projection measurements were obtained by compressing all sections from each z-stack into a single image, and measuring mean fluorescences of the entire cell areas.

In vivo assays

All procedures were licensed by UK Home Office and were carried out in accordance with local ethical review. 4-6 week old BALB/c nu/nu female mice (Charles River, UK) were injected subcutaneously with 1.5×10^6 LS174T cells to the flank. When tumours reached $\sim 10\text{mm}$ diameter, mice were randomised to either CEA-targeted or control IgG conjugated-nanoparticles (50mg/kg suspended in 100 μl PBS via tail vein under general anaesthesia). Fluorescent images were captured using IVIS imaging (filters: excitation 672nm, emission 694nm; Perkin Elmer, USA) under anaesthesia. Fluorescence measurements (radiant efficiency in $\text{p/sec/cm}^2/\text{sr}/\mu\text{W/cm}^2$) were taken using Living Image (v4.3.1, Caliper Life Sciences, USA); tumours were traced as regions of interest and mean quantum efficiency measurements taken, calibrated to background.

Statistics

Analyses were performed using in SPSS (SPSS, USA).

Results

Nanoparticle manufacture, antibody conjugation and physical characterisation

Protocols for manufacture of dye-doped silica nanoparticles encasing NIR664 dye were developed from published work [10, 11, 13]. Four separate protocols for conjugation of particles to antibodies were developed based on chemical linkers SMCC, PEG, EDC or PAMAM dendrimers, each of which has been reported to allow successful conjugation [13, 17-19]. A schematic of the particles is shown in Fig 1A. Particles were characterised using scanning electron microscopy (Fig 1B). Unconjugated particles had a mean diameter of 57nm and were relatively homogeneous (standard deviation 7nm), indicating that particles were consistently of a suitable size for intravenous delivery to tumours. Antibody-conjugated nanoparticles (data shown for PAMAM dendrimer-conjugated only) had an equally suitable mean diameter of 71nm.

PAMAM dendrimer-conjugation allows antibody-targeting of nanoparticles in vitro

We assessed whether our four conjugation strategies allowed targeting of nanoparticles to cancer cells using tumour-specific antibodies. Nanoparticles were conjugated to antibodies specific for either CEA, since this marker is highly sensitive and specific for colorectal cancer detection [7], or the glycoside digoxin, as a negative control. Binding of antibody-conjugated nanoparticles to three different colorectal cancer cell lines *in vitro* (LS174T, LoVo and HCT116) was quantified using confocal microscopy (Fig S1 and Fig 2). Fluorescence was first quantified on single optical sections through the middle of the cells. Nanoparticles conjugated using SMCC or PEG did not demonstrate any significant antibody-dependent tumour cell binding, although non-specific binding was seen with both CEA- and control IgG-targeted particles (Fig S1A and B). Similarly, nanoparticles conjugated using EDC showed very poor antibody-dependent tumour cell binding, with only 1.7-fold greater binding of CEA-targeted nanoparticles as compared to control in only one cell line (LoVo, $p=0.017$; Fig S1C). More encouragingly, conjugation via PAMAM dendrimers allowed strong tumour-specific targeting, with CEA-targeted nanoparticles demonstrating 12.3-, 8.0- and 3.2-fold greater fluorescence than control in LS174T, LoVo and HCT116 cells respectively ($p<0.002$; Fig 2A).

Fluorescence was also quantified throughout the depth of the cells using maximum projection images, which compress the signals seen in individual optical section into one image. A similar pattern of successful CEA-targeted fluorescence was observed ($p < 0.0002$; Fig 2B).

CEA-targeted nanoparticles allow in vivo fluorescent imaging of colorectal xenografts

Next, we assessed whether these nanoparticles would allow *in vivo* tumour imaging. LS174T xenografts were established in nude mice and mice were injected intravenously with either CEA-targeted nanoparticles ($n=3$) or control IgG nanoparticles ($n=3$). Fluorescence was quantified within specific organs/tissues (tumour or liver) non-invasively at time points from 1min through to 72h after injection. Hepatic fluorescence was observed in all mice, suggestive of hepatobiliary excretion, a feature observed previously [20]. Liver fluorescence was evident at 6h (mean 8.01×10^7 p/sec/cm²/sr/ μ W/cm²) and peaked at 24h (8.98×10^7 p/sec/cm²/sr/ μ W/cm²) before reducing (48h: 7.42×10^7 p/sec/cm²/sr/ μ W/cm² and 72h: 4.80×10^7 p/sec/cm²/sr/ μ W/cm²). Hepatic localisation was confirmed by *ex vivo* imaging of isolated organs. There was no significant difference in liver fluorescence between mice injected with control particles and those injected with CEA-targeted particles at any time point (p ranging from 0.3 to 0.9, Mann Whitney Test). Fluorescence in other mouse tissues was not seen for either control or CEA-targeted particles, demonstrating that the particles have negligible non-specific or antibody directed binding to host cells. Substantial tumour fluorescence was detected in all mice injected with CEA-targeted nanoparticles from 6h post-injection (Fig 3). Mean tumour fluorescence increased over the whole experiment from 6h (mean 0.62×10^7 p/sec/cm²/sr/ μ W/cm²) to 72h (mean 4.74×10^7 p/sec/cm²/sr/ μ W/cm²), although increases were only small after 48h. Mice injected with control IgG-targeted nanoparticles showed no tumour fluorescence above background at any point (Fig 3). Fluorescence in the CEA-targeted tumours was significantly greater than controls at every time point after and including 6h ($p < 0.0001$, Wilcoxon Signed Rank Test). The continued accumulation of tumour fluorescence with the CEA-targeted nanoparticles for up to 72h suggests that at least a proportion of the conjugated particles are stable in the circulation for a minimum of 72h.

Discussion

Dye-doped silica nanoparticles, as used here, were originally described in a study targeting human leukaemia cells *in vitro* [11]. The fluorescent nanoparticles were conjugated using cyanogen bromide to leukaemia cell-specific antibodies and the authors presented comparative images of cells incubated with targeted and control nanoparticles, although fluorescence was not quantified. However, critically, the controls consisted of ‘bare’ nanoparticles, with no targeting antibody or linkers attached, as opposed to the more appropriate controls of non-targeting antibodies. This lack of robust controls represents a key and recurring issue in the field, which is of particular importance since we show non-specific binding of antibody-conjugated nanoparticles is prevalent using some conjugation strategies (Fig S1) while antigen-specific targeting is more problematic.

Cyanogen bromide conjugation appears not to have been repeated in any other relevant work, however several groups have published studies with a variety of antibody-conjugations, including streptavidin-biotin [21], glutaraldehyde [10] and EDC [19, 22]. SMCC has also been used in similar contexts to conjugate reduced antibodies to nanoparticles using the free sulfhydryl group, with the aim of increasing specific targeting by improving antigen-recognition site orientation [17].

Conjugation using heterobifunctional PEG is a further option that can increase the particle circulating half-life by preventing reticulo-endothelial opsonisation [18]. More recently dendrimers have also been used as linkers between nanoparticles and antibodies [13]. We have tested four of these linkers, focusing on EDC, since this has been used in the overwhelming majority of studies, SMCC and PEG, on the basis of the potential advantages described above, and dendrimers. In order to test the abilities of these conjugations to direct antigen-specific binding of nanoparticles we have performed carefully controlled and quantified analyses. We have previously demonstrated that CEA is the most appropriate biomarker for targeting colorectal cancer cells [7]. Therefore, here, we have used colorectal cancer cells as a target for nanoparticles conjugated to anti-CEA antibodies or to anti-digoxin antibodies, with digoxin representing a negative-control antigen not present within these cells.

We found only dendrimers to allow target-specific nanoparticle binding in all colorectal cell lines (Fig 2). Notably, SMCC allowed fairly strong binding without any suggestion of specificity, while EDC allowed weak specific binding in only one cell line (Fig S1); these observations present concerns for the interpretation of previously published poorly-controlled studies.

Having developed a fluorescent nanoparticle with genuine specificity for a surface antigen that is over-expressed in cancers, we then examined the potential for this to be used to image tumours *in vivo*, using colorectal cancer xenografts. We delivered particles systemically to simulate a pre-operative intravenous injection. CEA-targeted particles demonstrated, using *in vivo* imaging, significant time-dependent accumulation within tumours that was entirely absent for control-targeted particles (Fig 3; $p < 0.0001$). Only two other studies have investigated specific targeting of dye-doped silica nanoparticles to tumours via systemic delivery: Tivnan et al [12] used dendrimer-conjugated particles targeted to neuroblastoma, whilst Soster et al [23] used PEG-conjugated particles targeted to colorectal cancer metastases, both in murine xenograft models. However, both studies used ‘bare’ nanoparticles as controls, which are potentially problematic in terms of demonstrating antigen-specific targeting, and both imaged fluorescence only on harvested organs *ex vivo*, which may relate to poor tissue penetration of fluorescence.

Conclusions

Our study is the first to use nanoparticles successfully to provide tumour-specific, live, *in vivo* fluorescent imaging in a murine model of colorectal cancer. Critically our work show great promise for clinical translation in the context of intra-operative imaging since fluorescence is bright, the antibody is humanised and has been used in clinical trials previously, and silica nanoparticles appear to have favourable toxicity profiles. Furthermore, the technology is applicable to imaging any tissue or pathology using antibodies targeting appropriate specific biomarkers.

Future perspective

Fluorescent laparoscopic imaging of primary colorectal tumours and lymph node metastases is likely to become a routine procedure during colorectal resections within the medium term. However, demonstrating specific tumour labelling remains problematic in many published studies. Further work is required using rigorous controls in order to optimise specific tumour labelling before such technologies can be translated into the clinic.

Executive summary

Background

- Colorectal surgery could be aided by fluorescent labelling of tumour cells

Materials and methods

- Dye-doped silica nanoparticles loaded with NIR664 dye were synthesised using a water-in-oil microemulsion technique
- Anti-CEA IgGs or control IgGs were conjugated to nanoparticles using a variety of chemical strategies, including polyamidoamine dendrimers (PAMAM).
- Binding of CEA-targeted or control nanoparticles to colorectal cancer cells (LS174T, LoVo and HCT116) was quantified *in vitro* using confocal microscopy, or *in vivo* in the context of a murine xenograft model using non-invasive IVIS imaging.

Results

- CEA-targeted, PAMAM dendrimer-conjugated, nanoparticles allowed strong tumour-specific targeting *in vitro*, demonstrating up to 12-fold greater fluorescence than control IgG-targeted nanoparticles ($p < 0.002$)
- CEA-targeted nanoparticles demonstrated clear tumour-specific fluorescence in xenografts from 6 to 72h after injection, as compared to only background fluorescence for control IgG-targeted nanoparticles ($p < 0.0001$)

Conclusion and future perspective

- These fluorescent nanoparticles show great promise for intra-operative imaging of colorectal cancers
- The same technology could be harnessed for specific labelling of other pathologies using appropriate antibodies

Acknowledgements

We thank the Biotherapeutics Development Unit (Clare Hall Laboratories, Cancer Research UK) for the A5B7 anti-CEA antibody. This work was supported by a CRUK fellowship to JPT, awarded through the Cancer Research UK Leeds Centre.

Figure legends

Figure 1 **A)** Schematic diagram of dye-doped silica nanoparticles conjugated to IgG antibodies via chemical linkers. 1 fluorescent core; 2 silica shell; 3 biochemical linker; 4 antibody. **B)** Field emission scanning electron microscope image of unconjugated particles (magnification, $\times 1 \times 10^5$). **C)** Diameters of 50 randomly-selected unconjugated particles or anti-CEA-conjugated particles were quantified from electron microscope images (means with standard deviations; significance tested using unpaired t-tests).

Figure 2 Dye-doped silica nanoparticles conjugated to anti-CEA antibodies via PAMAM dendrimers allow specific fluorescent imaging of colorectal cancer cell lines *in vitro*. Three different colorectal cancer cell lines were incubated with either nanoparticles conjugated to anti-CEA, or to control antibodies. Images were collected using confocal microscopy and fluorescence was quantified. Representative images are shown (magnification, $\times 63$): **A)** phase contrast and fluorescent central optical sections; **B)** phase contrast and maximum image projection. Graphs representing mean fluorescence (with standard deviations) are shown; significance was tested using unpaired t-tests.

Figure 3 CEA-targeted dye-doped silica nanoparticles allow live tumour-specific imaging *in vivo*. LS174T xenograft tumours were established in nu/nu balb-c mice. CEA-targeted or control IgG-conjugated particles were delivered systemically (50 mg/kg) and tumour fluorescence was measured using an IVIS small animal imaging system at the time points shown. Representative images are

shown of individual mice from each group (note these images were auto-exposed to enhance sensitivity, therefore depicted intensities are not comparable between images). Quantified data represent radiant efficiency for individual tumours in $\text{p/sec/cm}^2/\text{sr}/\mu\text{W/cm}^2$.

Figure S1 Antibody conjugation of dye-doped silica nanoparticles using SMC, PEG or EDC fails to allow consistent specific fluorescent imaging in LoVo cells. LoVo cells were incubated with either nanoparticles conjugated to either anti-CEA, or control antibodies using conjugation chemistry based on SMC, PEG or EDC as shown. Fluorescent images were collected using confocal microscopy and fluorescence was quantified. Representative phase contrast and fluorescent central optical section images are shown (magnification, x 63). Graphs representing mean fluorescence (with standard deviations) are shown; significance was tested using unpaired t-tests.

References

1. Jamieson JK, Dobson JF: The Lymphatics of the Colon. *Proc R Soc Med* 2(Surg Sect), 149-174 (1909).
2. Baxter NN, Virnig DJ, Rothenberger DA, Morris AM, Jessurun J, Virnig BA: Lymph node evaluation in colorectal cancer patients: A population-based study. *Journal of the National Cancer Institute* 97(3), 219-225 (2005).
3. Logan RFA, Patnick J, Nickerson C, Coleman L, Rutter MD, Von Wagner C: Outcomes of the Bowel Cancer Screening Programme (BCSP) in England after the first 1 million tests. *Gut*, (2011).
4. Hohenberger W, Weber K, Matzel K, Papadopoulos T, Merkel S: Standardized surgery for colonic cancer: complete mesocolic excision and central ligation - technical notes and outcome. *Colorectal Disease* 11(4), 354-364 (2009).
5. Association of Coloproctology of Great Britain and Ireland: National Bowel Cancer Audit Annual Report 2013. (2013).
6. Cahill R, Anderson M, Wang L, Lindsey I, Cunningham C, Mortensen N: Near-infrared (NIR) laparoscopy for intraoperative lymphatic road-mapping and sentinel node identification during definitive surgical resection of early-stage colorectal neoplasia. *Surgical Endoscopy* 26(1), 197-204 (2012).
7. Tiernan JP, Perry SL, Verghese ET *et al.*: Carcinoembryonic antigen is the preferred biomarker for in vivo colorectal cancer targeting. *British Journal of Cancer* 108(3), 662-667 (2013).
8. Weissleder R: A clearer vision for in vivo imaging. *Nat. Biotechnol.* 19(4), 316-317 (2001).
9. Mank AJG, Yeung ES: DIODE LASER-INDUCED FLUORESCENCE DETECTION IN CAPILLARY ELECTROPHORESIS AFTER PRECOLUMN DERIVATIZATION OF AMINO-ACIDS AND SMALL PEPTIDES. *Journal of Chromatography A* 708(2), 309-321 (1995).
10. Huang S, Li R, Qu Y, Shen J, Liu J: Fluorescent Biological Label for Recognizing Human Ovarian Tumor Cells Based on Fluorescent Nanoparticles. *Journal of Fluorescence* 19(6), 1095-1101 (2009).
11. Santra S, Zhang P, Wang KM, Tapeç R, Tan WH: Conjugation of biomolecules with luminophore-doped silica nanoparticles for photostable biomarkers. *Analytical Chemistry* 73(20), 4988-4993 (2001).
12. Tivnan A, Orr WS, Gubala V *et al.*: Inhibition of Neuroblastoma Tumor Growth by Targeted Delivery of MicroRNA-34a Using Anti-Disialoganglioside GD(2) Coated Nanoparticles. *Plos One* 7(5), (2012).
13. Gubala V, Le Guevel X, Nooney R, Williams DE, Macraith B: A comparison of mono and multivalent linkers and their effect on the colloidal stability of nanoparticle and immunoassays performance. *Talanta* 81(4-5), 1833-1839 (2010).
14. Harwood PJ, Britton DW, Southall PJ, Boxer GM, Rawlins G, Rogers GT: Mapping epitope characteristics on carcinoembryonic antigen. *Br. J. Cancer* 54(1), 75-82 (1986).
15. Dawson PM, Blair SD, Begent RH, Kelly AM, Boxer GM, Theodorou NA: The value of radioimmunoguided surgery in first and second look laparotomy for colorectal cancer. *Diseases of the colon and rectum* 34(3), 217-222 (1991).
16. Meyer T, Gaya AM, Dancey G *et al.*: A phase I trial of radioimmunotherapy with ¹³¹I-A5B7 anti-CEA antibody in combination with combretastatin-A4-phosphate in advanced gastrointestinal carcinomas. *Clin Cancer Res* 15(13), 4484-4492 (2009).
17. Lee J, Choi Y, Kim K *et al.*: Characterization and Cancer Cell Specific Binding Properties of Anti-EGFR Antibody Conjugated Quantum Dots. *Bioconjugate Chemistry* 21(5), 940-946 (2010).

18. Owens IJ DE, Peppas NA: Opsonization, biodistribution, and pharmacokinetics of polymeric nanoparticles. *International Journal of Pharmaceutics* 307(1), 93-102 (2006).
19. Zhao XJ, Hilliard LR, Mechery SJ *et al.*: A rapid bioassay for single bacterial cell quantitation using bioconjugated nanoparticles. *Proceedings of the National Academy of Sciences of the United States of America* 101(42), 15027-15032 (2004).
20. Souris JS, Lee C-H, Cheng S-H *et al.*: Surface charge-mediated rapid hepatobiliary excretion of mesoporous silica nanoparticles. *Biomaterials* 31(21), 5564-5574 (2010).
21. Lian W, Litherland SA, Badrane H *et al.*: Ultrasensitive detection of biomolecules with fluorescent dye-doped nanoparticles. *Analytical Biochemistry* 334(1), 135-144 (2004).
22. Wu H, Huo Q, Varnum S *et al.*: Dye-doped silica nanoparticle labels/protein microarray for detection of protein biomarkers. *Analyst* 133(11), 1550-1555 (2008).
23. Soster M, Juris R, Bonacchi S *et al.*: Targeted dual-color silica nanoparticles provide univocal identification of micrometastases in preclinical models of colorectal cancer. *International Journal of Nanomedicine* 7, 4797-4807 (2012).

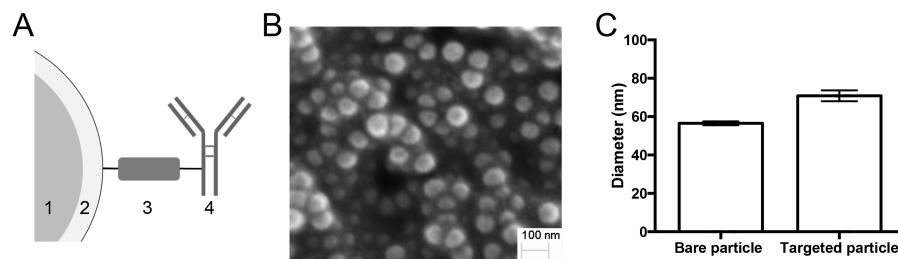


Fig 1

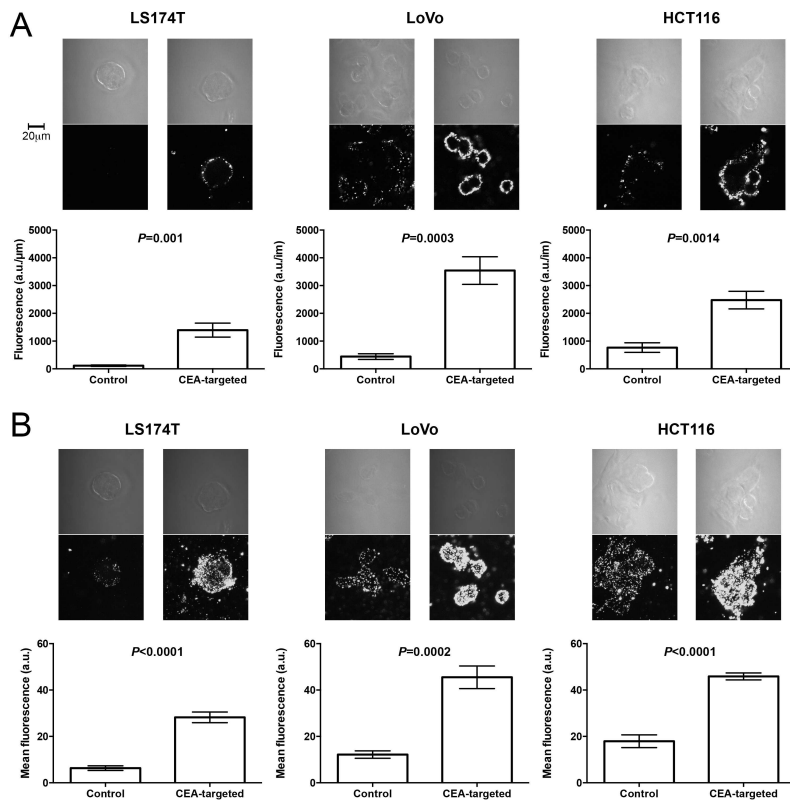


Fig 2

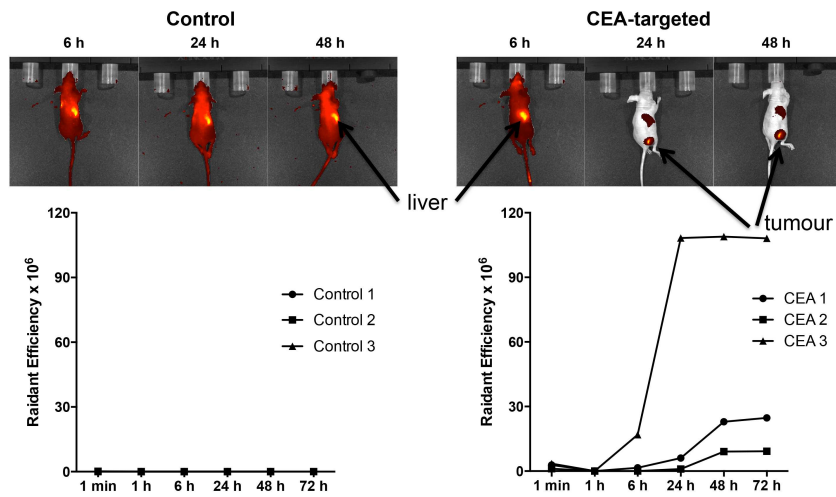


Fig 3